

MAPPING AND MORPHOMETRY OF LARGE IMPACT FEATURES ON GANYMEDE AND CALLISTO. O. L. White^{1,2}, P. M. Schenk³, D. G. Korycansky⁴, J. M. Moore², A. J. Dombard⁵, M. Caussi⁵. ¹SETI Institute, Mountain View, CA, 94043 (owhite@seti.org), ²NASA Ames Research Center, Moffett Field, CA, 94035, ³Lunar and Planetary Institute, Houston, TX, 77058, ⁴University of California, Santa Cruz, CA, 95064, ⁵University of Illinois at Chicago, Chicago, IL, 60607.

Introduction: The icy Galilean satellites (Ganymede, Callisto, Europa) are host to a variety of large impact features that are, if not unique to these bodies, rarely encountered on planetary and satellite surfaces in the Solar System. These features are morphologically diverse and include impact craters with central pits and domes, and so-called "penepalimpsests" and "palimpsests", which appear as circular albedo features with negligible topographic relief and absent crater rims [1-4]. The particular properties of the formation of these impact features are likely governed by the interplay of several factors that may include the presence or absence of liquid water (at depth below the surface, or generated during the impact) vs. warm ice (again, either pre-existing or impact-generated) [2,5-8]; the lithospheric temperature gradient [9]; surface gravity (as compared to smaller gravity on mid-sized satellites, where the features of interest are not found); and the characteristics of the impactor, specifically the impactor's size, velocity, composition, and the angle of impact. We are evaluating specific and testable hypotheses about the role of each of these factors in the formation and evolution of impact features. This is being accomplished through geological and topographic mapping of selected impact features, which serve as primary ground-truth for numerical modeling of the impact process. Here, we present general observations from the mapping and associated morphometry.

Generation of Maps and Digital Elevation Models: Localized base maps assembled from Voyager and Galileo images have been generated for 20 impact features on Ganymede and Callisto (17 on Ganymede and 3 on Callisto). Where data allows, we have also generated digital elevation models (DEMs) for impact features using stereo photogrammetry and photoclinometry (shape-from-shading). The impact features, listed in Table 1, are representative of the full range of large impact feature morphologies. Our geologic mapping of these features uses DEMs iteratively with the base maps to identify crater facies. For mapped impact features that have associated DEMs, we have produced averaged profiles of the features and collected morphometric statistics of mapped units, including but not limited to the diameters, depths/heights, and volumes of craters, central pits, and domes. We will use these statistics to quantitatively compare impact feature morphology and constrain and rank-order competing hypotheses for their formation and evolution.

Table 1. List of 20 mapped impact features on Ganymede and Callisto.

Impact feature name and parent satellite	Diameter (km)	Morphological class
Achelous (G)	40	Pit crater
Lugalmeslam (G)	64	Pit crater
Isis (G)	75	Pit crater
Tindr (C)	76	Pit crater
Eshmun (G)	101	Dome crater
Melkart (G)	104	Dome crater
Osiris (G)	107	Dome crater
Anubis (G)	114	Dome crater
Doh (C)	76 (annulus)	Anomalous dome crater
Har (C)	110 (platform)	Anomalous dome crater
Neith (G)	170	Anomalous dome crater
Anzu (G)	193	Anomalous dome crater
Serapis (G)	253	Anomalous dome crater
Hathor (G)	173	Penepalimpsest
Buto (G)	235	Penepalimpsest
Nidaba (G)	265	Penepalimpsest
Teshub (G)	188	Palimpsest
Zakar (G)	265	Palimpsest
Epigeus (G)	349	Palimpsest
Memphis (G)	354	Palimpsest

Mapping and morphometry results: Fig. 1 presents mapping and topography of 4 impact features, one each from the pit crater (Tindr), dome crater (Melkart), anomalous dome crater (Neith), and penepalimpsest (Hathor) morphological classes. All features belonging to the crater morphological classes show a configuration of a central pit (or in the case of the smaller features like Tindr, multiple small pits), surrounded by a hummocky annulus that for larger features (like Neith) develops into a system of radial, elevated ridges separated by valleys extending outwards from the pit. The annulus is surrounded by an expanse of smooth plains corresponding to the crater floor, which in turn is surrounded by an outer rim that tends to be quite narrow and attain high relief for pit and dome craters, but becomes much broader and muted for anomalous dome craters. Domes start to appear

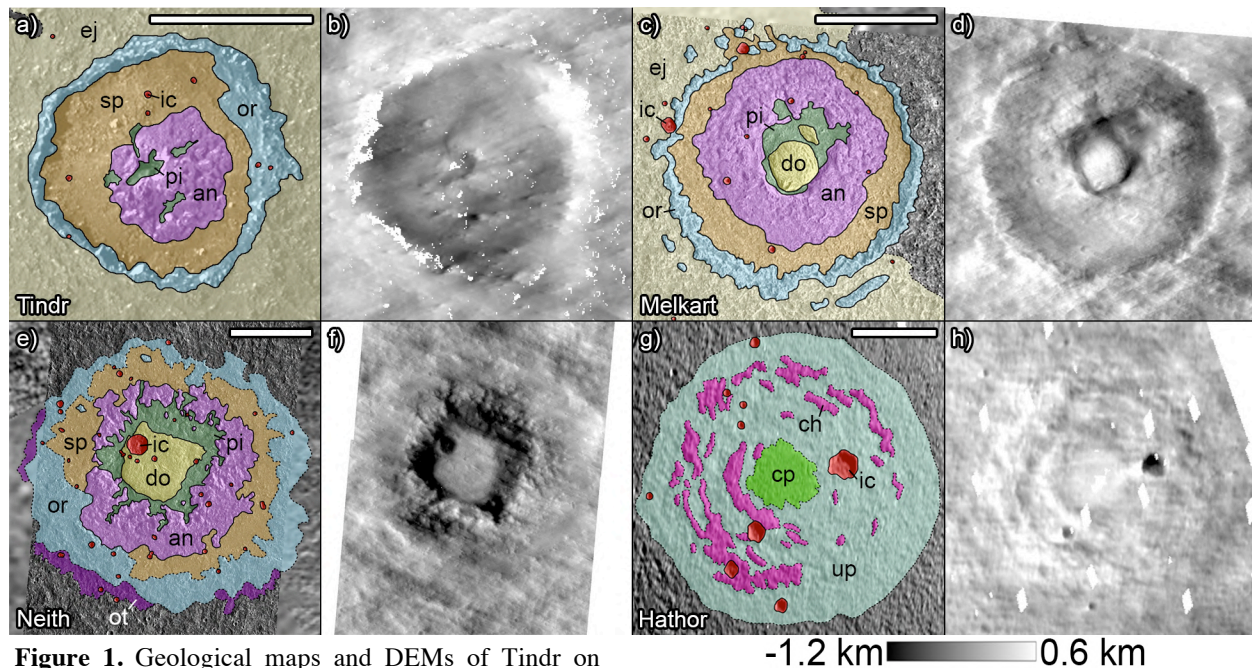


Figure 1. Geological maps and DEMs of Tindr on Callisto and Melkart, Neith, and Hathor on Ganymede. Unit labels are as follows: ic = impact crater; do = dome; pi = central pit; an = annulus; sp = smooth plains; or = outer rim; ot = outer trough; ej = ejecta; cp = central plains; ch = concentric hills; up = undulating plains. Scale bars all measure 50 km. DEMs are all shown to the same elevation scale (shown at right).

within the central pit as the ratio of pit diameter to outer rim diameter exceeds 0.4. The ratio of the volumes of these domes relative to the volumes of the pits in which they are contained tends to be towards the lower end of the range of 0.15 to 0.55, but Melkart's dome is remarkable in that its very high dome (rising 1.36 km above its base compared to the mean of 0.8 km) has essentially the same volume as its pit. For pit craters, the ratio of crater volume to pit volume decreases as pit morphology transitions from several small pits within the annulus (Achelous and Tindr) to a single pit surrounded by the annulus (Lugalmeslam and Isis), and then lower still with the transition to dome craters. For anomalous dome craters, with prominent central pits but very subdued crater floors, the pit volume can exceed that of the crater itself (as in the case of Neith).

Serapis and Hathor represent a transition from anomalous dome craters to penepalimpsests. The essential elements of anomalous dome craters can be recognized in Serapis, but its annulus appears to be dissociating into a fragmented, concentric configuration. For Hathor, this transition has advanced such that it presents a set of concentric chains of hills surrounding an expanse of smooth plains at the center. The majority of the impact feature consists of undulating

plains, with no identifiable rim, crater floor, or central pit. In Hathor's case the smooth central plains superpose the surrounding undulating plains and are raised by ~400 m above them, but do not constitute an actual dome. For larger penepalimpsests, these central plains are not raised above the surroundings, suggesting that Hathor's central plains might represent a rheological transition between a dome and the lower lying central plains of larger palimpsest-type features. We refer the reader to these abstracts for further details of mapping and morphometry results on these satellites, as well as modeling work informed by it [10-14].

Acknowledgements: This research has been funded by NASA's SSW award 80NSSC19K0551.

References: [1] Passey Q. R. & Shoemaker E. M. (1982) In *Satellites of Jupiter*, pp. 379-434, University of Arizona Press. [2] Moore J. M. & Malin M. C. (1988) *Geophys. Res. Lett.*, 15, 225-228. [3] Schenk P. M. & Moore J. M. (1998) In *Solar System Ices*, pp. 551-578, Springer. [4] Schenk P. M. et al. (2004) In *Jupiter: The Planet, Satellites and Magnetosphere*, pp. 427-456, Cambridge University Press. [5] Croft S. K. (1983) *J. Geophys. Res.*, 88, 71-89. [6] Schenk P. M. (1993) *J. Geophys. Res. Planets*, 98, 7475-7498. [7] Schenk P. M. (2010) *Atlas of the Galilean Satellites*, 394 pp., Cambridge University Press. [8] Senft L. E. & Stewart S. T. (2011) *Icarus*, 214, 67-81. [9] Bray V. J. et al. (2014) *Icarus*, 231, 394-406. [10] Moore J. M. et al. (2022) *LPSC LIII*, Abstract #1643. [11] Caussi M. et al. (2022) *LPSC LIII*, Abstract #2164. [12] Korycansky D. G. et al. (2022) *LPSC LIII*, Abstract #1309. [13] Korycansky D. G. et al. (2022) *LPSC LIII*, Abstract #1310. [14] Schenk P. M. et al. (2022) *LPSC LIII*, *ibid.*